Contribution from the Dipartimento di Chimica, Università di Modena, 41100 Modena, Italy, Istituto di Chimica Generale e Inorganica, Centro di Studio per la Strutturistica Diffrattometrica del CNR, Università di Parma, 43100 Parma, Italy, and Departments of Chemistry, Università degli Studi di Firenze, 50121 Firenze, Italy, Washington State University, Pullman, Washington 99164, and Illinois State University, Normal, Illinois 61761

Crystal Structure, Thermal Properties, and Spectroscopy of $(H_2Me_2pipz)[CuCl_3(H_2O)]_2$ (H_2Me_2pipz = *N*,*N*'-Dimethylpiperazinium) and (HAmpym)$[CuCl_3(H_2O)]$ (HAmpym = 2-Aminopyrimidinium)

Tiziano Manfredini,[†] Gian Carlo Pellacani,*[,†] Anna Bonamartini-Corradi,[‡] Luigi Pietro Battaglia,[‡] Giulio G. T. Guarini,[§] Jolanda Gelsomini Giusti,[§] George Pon,[∥] Roger D. Willett,*[,∥] and Douglas X. West[⊥]

Received December 8, 1988

The crystal structures of two hydrated copper(II) chloride salts are reported: *N*,*N*'-dimethylpiperazinium bis(aquotrichlorocuprate(II)), $C_6H_{20}N_2O_2Cu_2Cl_6$, monoclinic, $P2_1/n$, a = 6.714 (2) Å, b = 6.215 (2) Å, c = 19.545 (6) Å, β = 92.24 (6)°, Z = 2, and R = 0.041, and 2-aminopyrimidinium aquotrichlorocuprate(II), $C_4H_8N_3OCuCl_3$, monoclinic, Cc, a = 3.9025 (6) Å, b = 13.788 (3) Å, c = 16.826 (3) Å, β = 93.99 (1)°, Z = 4, and R = 0.030. In addition, the crystal parameters of the anhydrous analogue of the latter, bis(2-aminopyrimidinium) hexachlorodicuprate(II), $C_8H_{12}N_6Cu_2Cl_6$ are triclinic, a = 3.902 (1) Å, b = 10.850 (3) Å, c = 11.129 (3) Å, α = 62.82 (2)°, β = 84.84 (3)°, γ = 82.69 (2)°, Z = 1, and R = 0.0252. Both hydrated structures contain planar $CuCl_3(H_2O)^-$ anions linked together by longer (~3.1 Å) semicoordinate Cu···Cl bonds to form stacks. In the first salt, stacks are linked together by O-H···Cl hydrogen bonds to form planes, with the planes bridged by hydrogen-bonded piperazinium cations. In the latter salt, the stacks are tied together into a tight three-dimensional network by O-H···Cl, N-H···Cl, and N···H···O hydrogen bonds. A comparison of these patterns with those of other stacked CuL_4 species is given. The anhydrous pyrimidinium salt contains stacks of planar, bibridged $Cu_2Cl_6^{2-}$ anions. Electronic, IR, and EPR spectra of the hydrated species are consistent with the observed Cu(II) coordination. Both compounds exhibit weak antiferromagnetic exchange coupling. Detailed analysis for the pyrimidinium salt yields an intrachain coupling of J/k = 3.1 (1) K and interchain couplings of $J'/k \sim 0.1$ K and $|J''/k| < 0.01$ K. The thermal stability of both salts has been investigated by DSC and TGA measurements. Single crystals of the piperazinium salt begin surface dehydration at 95 °C, initiating conversion to a red solid, with a phase transition to the red solid at 140 °C. Single crystals of the pyrimidinium salt undergo a dehydration at 80 °C, converting to a red solid by 110 °C. This is followed at 120 °C by a phase transition to a yellow solid.

Introduction

The structural properties of copper(II) halides continue to be of interest, primarily because of the wide variety of stereochemical features as well as complex and unexpected oligomeric species.[1] Among the monomeric $CuCl_{n+2}^{n-}$ complexes, only square-planar,[2] distorted tetrahedral,[3] or square-pyramidal[4] anions are known. The trigonal-bipyramidal $CuCl_5^{3-}$, originally thought to exist in $Co(NH_3)_6CuCl_5$,[5a] has been shown to be an artifact due to the presence of square-pyramidal ions disordered about 3-fold axes in the structure.[5b] The isolated square-planar $CuCl_4^{2-}$ anion exists in numerous salts that are usually, but not always, stabilized by cation-Cl hydrogen bonding. In the antiferrodistortive $(RNH_3)_2CuCl_4$ salts,[5] two longer semicoordinate bonds are formed to give a strongly elongated 4 + 2 distorted octahedral coordination. Planar coordination also exists in a number of $CuCl_2L_2$ systems,[6] where L is a ligand that is not very bulky. In this case, the $CuCl_2L_2$ species aggregate into stacks[1c] (I-III), again through

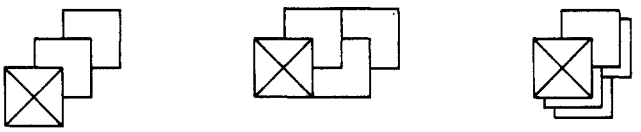

I II III

the formation of two semicoordinate bonds (when only one semicoordinate bond exists, the species dimerize with resultant distortion of the primary planar coordination[7]). A few $CuCl_3L^-$ ions are also known,[8] but with L = H_2O, the only known $CuCl_3(H_2O)^-$ anion occurs as a weakly coordinating counterion in $[Cu_2(3,6\text{-bis}(1\text{-pyrazolyl})\text{pyridazine})(OH)Cl_2]CuCl_3(H_2O)$.[8c] In contrast, the $CuCl_2(H_2O)_2$ species has been reported in $CuCl_2{\cdot}2H_2O$,[6a] in $(pyNO)_2Cu_3Cl_6{\cdot}2H_2O$,[9a] and in $(C_7H_7N)_2CuCl_4{\cdot}H_2O$.[9b] The preponderance of $CuCl_2L_2$ species, as contrasted to $CuCl_3L^-$ species, might imply some preferred thermodynamic stability for the former. Nonetheless, three planar $Cu_2Cl_5(H_2O)^-$ dimers have recently been reported,[10] so it would appear that the monoaquo species should not be inherently thermodynamically unstable.

In this paper, we report on the preparation and the structural, spectroscopic, and stability properties of two salts containing the planar $CuCl_3(H_2O)^-$ anion. The stacking of these anions is compared to the stacking of other planar monomers previously observed. The role of the water molecule in stabilizing the

[†] Universita di Modena.
[‡] Universita di Parma.
[§] Universita degli Studi di Firenze.
[∥] Washington State University.
[⊥] Illinois State University.

(1) (a) Smith, D. W. *Coord. Chem. Rev.* **1976**, *21*, 93. (b) Willett, R. D.; Geiser, U. *Croat. Chim. Acta* **1984**, *57*, 737. (c) Geiser, U.; Willett, R. D.; Lindbeck, M.; Emerson, J. *J. Am. Chem. Soc.* **1986**, *108*, 1173. Bond, M. R.; Willett, R. D. *Inorg. Chem.* **1989**, *28*, 3267.
(2) Harlow, R. L.; Wells, W. J., III; Watt, G. W.; Simonsen, S. H. *Inorg. Chem.* **1974**, *13*, 2106. Nelson, H. C.; Simonsen, S. H.; Watt, G. W. *J. Chem. Soc., Chem. Commun.* **1979**, *632*. Udupa, M. R.; Krebs, B. *Inorg. Chim. Acta* **1979**, *33*, 241.
(3) Dyrek, K.; Gosler, J.; Hodorowicz, S. A.; Hoffmann, S. K.; Oleksyn, B. J.; Weselucha-Brczynska, A. *Inorg. Chem.* **1987**, *26*, 1481 and references therein.
(4) Antolini, L.; Marcotrigiano, G.; Menabue, L.; Pellacani, G. C. *J. Am. Chem. Soc.* **1980**, *102*, 1303.
(5) Steadman, J. P.; Willett, R. D. *Inorg. Chim. Acta* **1970**, *4*, 367.
(6) (a) Harker, D. *Z. Kristallogr.* **1936**, *93*, 136. (b) Morosin, B. *Acta Crystallogr.* **1975**, *B31*, 632.
(7) Hatfield, W. E.; ter Haar, L. W.; Olmstead, M. M.; Musker, W. K.; *Inorg. Chem.* **1986**, *25*, 558 and references therein.
(8) (a) Brown, D. B.; Donner, J. A.; Hall, J. W.; Wilson, S. R.; Wilson, R. B; Hodgson, D. J.; Hatfield, W. E. *Inorg. Chem.* **1979**, *18*, 2635. (b) Trotter, J.; Whitlow, S. H. *J. Chem. Soc. A* **1966**, 455. (c) Thompson, L. K.; Woon, T. C.; Murphy, D. B.; Gabe, E. J.; Lee, F. L.; LePage, Y. *Inorg. Chem.* **1985**, *24*, 4719.
(9) (a) Sager, R. S.; Watson, W. H. *Inorg. Chem.* **1968**, *7*, 2035. (b) Bukowska-Strzyzewska, M.; Skoweranda, J. *Acta Crystallogr., Sect. C* **1987**, *C43*, 2290.
(10) (a) Bond, M. R.; Willett, R. D. *Acta Crystallogr., Sect. C* **1988**, *C43*, 2304. (b) Bond, M. R.; Willett, R. D. *J. Am. Chem. Soc.*, in preparation.
(11) Sheldrick, G. *SHELXTL version 5.1*; Nicolet Instrument Co.: Madison, WI, 1986.
(12) Campana, C. F.; Shepherd, D. F.; Litchman, W. N. *Inorg. Chem.* **1981**, *20*, 4039.
(13) *International Tables for X-ray Crystallography*; Press: Birmingham, England, 1983; Vol. VI.

0020-1669/90/1329-2221$02.50/0

Table I. Crystallographic Data

compd	$(H_2Me_2pipz)[CuCl_3(H_2O)]_2$	$(HAmpym)[CuCl_3(H_2O)]$	$(HAmpym)_2Cu_2Cl_6$
formula	$C_6H_{20}Cl_6Cu_2N_2O_2$	$C_4H_8Cl_3CuN_3O$	$C_8H_{12}Cl_6Cu_2N_6$
fw	492.05	314.5	532.01
cryst class	monoclinic	monoclinic	triclinic
space group	$P2_1/n$	Cc	$P\bar{1}$
a, Å	6.714 (2)	3.9025 (6)	3.902 (1)
b, Å	6.215 (2)	13.788 (3)	10.850 (3)
c, Å	19.545 (6)	16.826 (3)	11.129 (3)
α, deg			62.82 (2)
β, deg	95.2 (6)	93.99 (1)	84.84 (2)
γ, deg			82.69 (2)
V, Å^3	812.1 (2)	903.2 (1)	415.4 (2)
Z	2	4	1
T, °C	22	22	21
λ, Å	0.71069	0.71069	0.71069
ρ_{calc}, g/cm^3	2.01	2.09	2.13
μ, cm^{-1}	36.2	32.7	35.4
transm	0.0682–1.000	0.294–0.362	0.698–0.970
$R(F_o)$	0.041	0.0305 (0.0347, all)	0.0252 (0.0266, all)
$R_w(F_o)$	0.052	0.0385 (0.0392, all)	0.0381 (0.0389, all)

Table II. Atomic Coordinates (×10^4) and Equivalent Isotropic Thermal Parameters (×10^3) for $(H_2Me_2pipz)(CuCl_3(H_2O)_2)$

atom	x	y	z	U_{eq}, Å^2
Cu	2086 (1)	3970 (1)	8038 (1)	17 (1)
Cl(1)	1026 (1)	3895 (2)	9100 (1)	30 (1)
Cl(2)	5390 (2)	3592 (2)	8438 (1)	30 (1)
Cl(3)	2878 (2)	3974 (2)	6935 (1)	39 (1)
O	−746 (6)	4483 (8)	7645 (2)	36 (3)
N	3891 (6)	386 (7)	588 (2)	24 (2)
C(1)	5218 (7)	2085 (8)	324 (3)	25 (3)
C(2)	3092 (8)	−1061 (9)	10 (3)	28 (3)
C(3)	2203 (11)	1393 (11)	949 (4)	38 (4)

Table III. Atomic Coordinates (×10^4) and Equivalent Isotropic Thermal Parameters (×10^3) for $(HAmpym)CuCl_3(H_2O)$

atom	x	y	z	U_{eq}, Å^2
Cu	9954	−7384 (1)	1009	23 (1)
Cl(1)	13413 (2)	−7242 (1)	8972 (1)	29 (1)
Cl(2)	10281 (2)	−5780 (1)	10295 (1)	25 (1)
Cl(3)	6853 (2)	−7708 (1)	11084 (1)	29 (1)
O	9762 (6)	−8793 (1)	9780 (1)	31 (1)
N(7)	2146 (6)	−6633 (2)	12496 (1)	30 (1)
C(1)	4173 (5)	−5860 (1)	12524 (1)	22 (1)
N(2)	5047 (5)	−5439 (1)	11840 (1)	24 (1)
C(3)	6931 (6)	−4619 (2)	11842 (1)	26 (1)
C(4)	8091 (6)	−4215 (2)	12551 (1)	28 (1)
C(5)	7231 (6)	−4692 (2)	13243 (1)	27 (1)
N(6)	5312 (5)	−5489 (1)	13238 (1)	25 (1)

Table IV. Atomic Coordinates (×10^4) and Isotropic Thermal Parameters (×10^3) for $(HAmpym)_2Cu_2Cl_6$

atom	x	y	z	U, Å^2
Cu	2149 (1)	3330 (1)	741 (1)	24 (1)
Cl(1)	1306 (2)	5320 (1)	1084 (1)	25 (1)
Cl(2)	5942 (2)	2307 (1)	2403 (1)	31 (1)
Cl(3)	3147 (2)	1609 (1)	79 (1)	27 (1)
N(2)	2078 (6)	6544 (2)	4752 (2)	27 (1)
Cl(1)	2997 (7)	6977 (3)	3438 (3)	24 (1)
N(6)	1696 (6)	8214 (3)	2491 (2)	32 (1)
N(7)	5251 (6)	6168 (3)	3083 (2)	33 (1)
C(3)	−68 (7)	7393 (3)	5077 (3)	32 (1)
C(5)	−494 (7)	9098 (3)	2814 (3)	35 (1)
C(4)	−1409 (8)	8711 (3)	4131 (3)	37 (1)

Table V. Anion Bond Lengths (Å) and Angles (deg) for $(H_2Me_2pipz)(CuCl_3(H_2O))_2$[a]

Distances			
Cu–Cl(1)	2.255 (3)	Cu–Cl(3b)	3.106 (2)
Cu–Cl(2)	2.296 (2)	O–Cl(2c)	3.190 (5)
Cu–Cl(3)	2.267 (3)	O–Cl(2a)	3.339 (5)
Cu–O	2.010 (4)	N–Cl(2d)	3.131 (5)
Cu–Cl(3a)	3.110 (2)		

Angles			
Cl(1)–Cu–Cl(2)	93.5 (2)	Cl(2)–Cu–O	175.8 (2)
Cl(1)–Cu–Cl(3)	175.1 (2)	Cl(3)–Cu–O	86.1 (2)
Cl(1)–Cu–O	89.3 (3)	Cu–Cl(3a)–Cu(a)	89.1 (1)
Cl(2)–Cu–Cl(3)	91.2 (2)	Cu–Cl(3b)–Cu(b)	89.3 (1)

[a] Coordinate transformation key: (a) $^1/_2 - x, ^1/_2 + y, ^3/_2 - z$; (b) $^1/_2 - x, -^1/_2 + y, ^3/_2 - z$; (c) $-1 + x, y, z$; (d) $1 - x, -y, 1 - z$.

structures through hydrogen bonding is explored, particularly with reference to their thermal stability.

Experimental Details

$(HAmpym)CuCl_3 \cdot H_2O$ (HAmpym = 2-aminopyrimidinium) was prepared by dissolving an equal molar mixture of 2-aminopyrimidine and $CuCl_2 \cdot 2H_2O$ in a small amount of hot 6 M HCl solution and allowing the solution to cool. Green crystals of some size (several millimeters on a side) were readily obtained under normal cooling rates. If crystallization occurred while the solution was too warm or if the acid concentration was too high, bright yellow crystals of $(HAmpym)_2CuCl_4$ were obtained initially. In such instances, dilute HCl solution was added to lower the concentration sufficiently so that initial crystallization occurred at a temperature where the monohydrate was the stable species in equilibrium with solution. Evaporation of the hot 9 M HCl solution at elevated temperature ($T > 50$ °C) yields red crystals of the anhydrous $(HAmpym)_2Cu_2Cl_6$ salt. $(H_2Me_2pipz)(CuCl_3 \cdot H_2O)_2$ (H_2Me_2pipz = *N,N'*-dimethylpiperazinium) was prepared in a similar fashion from dilute (1–3 M HCl) solutions containing a 1:2 ratio of the organic cation to $CuCl_2 \cdot 2H_2O$. For both hydrated salts, slow evaporation of a saturated solution at room temperature yielded crystals of up to 0.5 cm on an edge and up to 1 mm in thickness.

Crystal structures of the *N,N'*-dimethylpiperazinium salt and of the 2-aminopyrimidinium salts were determined at Parma, Italy, and Pullman, WA, respectively. The data for the former were collected on a Philips PW1100 diffractometer, and the SHELX package was used to solve the structure by utilizing a GOULD 32177 computer. The latter data collections were performed with a Syntex $P2_1$ diffractometer upgraded to Nicolet P3F specifications and the structure determinations carried out on a Data General Eclipse S240 computer with the SHELXTL program package. Important crystal parameters and refinement results are given in Table I for all three compounds. Refinements proceeded in a straightforward manner. For the piperazinium salt, the positional and isotropic thermal parameters were varied for all hydrogen atoms. The positional parameters of the water and amine protons were allowed to vary in the hydrated pyrimidinium salt; the ring protons affixed to carbon atoms were fixed at calculated positions. Isotropic thermal parameters for protons involved in hydrogen bonding were varied. One proton was found to be disordered between the oxygen atom and a ring nitrogen, N(6), and its occupancy factor was arbitrarily fixed at a value of 0.5. In the anhydrous pyrimidinium salt, the proton positions were assigned on the basis of electron difference maps. The C–H protons were fixed at ideal geometry, the positional and an isotropic thermal parameter were varied for the ring N–H proton (final N(6)–H(6) distance = 0.78 (4) Å), and a 2-fold disorder was assumed for the amino protons. Final atom coordinates and equivalent isotropic thermal parameters are listed in Tables II–IV, respectively, and pertinent bond distances and angles are given in Tables V–VII. Complete listings of data collection and refinement parameters, hydrogen atom positions, anisotropic thermal pa-

Table VI. Anion Bond Lengths (Å) and Angles (deg) for $(HAmpym)CuCl_3(H_2O)$[a]

	Distances		
Cu-Cl(1)	2.287 (1)	O-N(6c)	2.807 (4)
Cu-Cl(2)	2.265 (1)	O-Cl(2b)	3.396 (2)
Cu-Cl(3)	2.288 (1)	N(7)-Cl(3)	3.444 (2)
Cu-O	1.982 (2)	N(7)-Cl(3b)	3.385 (2)
Cu-Cl(1a)	2.996 (1)	N(7)-Cl(1d)	3.353 (2)
Cu-Cl(3b)	3.169 (1)	N(2)-Cl(2)	3.455 (2)
	Angles		
Cl(1)-Cu-Cl(2)	92.9 (1)	Cl(2)-Cu-O	178.6 (1)
Cl(1)-Cu-Cl(3)	172.7 (1)	Cl(3)-Cu-O	87.0 (1)
Cl(2)-Cu-Cl(3)	92.7 (1)	Cu-Cl(1a)-Cu(a)	94.3 (1)
Cl(1)-Cu-O	87.2 (1)	Cu-Cl(3b)-Cu(b)	89.8 (1)

[a] Coordinate transformation key: (a) $1 + x, y, z$; (b) $-1 + y, y, z$; (c) $-0.5 + x, -1.5 - y, 0.5 + z$; (d) $0.5 + y, -1.5 - y, -0.5 + z$.

Table VII. Bond Lengths (Å) and Angles (deg) for $(HAmpym)_2Cu_2Cl_6$

	Distances		
Cu-Cl(1)	2.338 (1)	N(2)-C(3)	1.317 (4)
Cu-Cl(2)	2.245 (1)	C(1)-N(6)	1.342 (3)
Cu-Cl(3)	2.280 (1)	C(1)-N(7)	1.325 (4)
Cu-Cl(1a)	2.316 (1)	N(6)-C(5)	1.352 (4)
Cu-Cl(1b)	3.177 (1)	C(3)-C(4)	1.400 (4)
Cu-Cl(2b)	2.919 (1)	C(5)-C(4)	1.355 (5)
N(2)-C(1)	1.345 (3)		
	Angles		
Cl(1)-Cu-Cl(2)	91.1 (1)	N(2)-C(2)-N(6)	121.0 (3)
Cl(1)-Cu-Cl(3)	171.5 (1)	N(2)-C(1)-N(7)	119.0 (2)
Cl(2)-Cu-Cl(3)	94.0 (1)	N(6)-C(1)-N(7)	119.9 (2)
Cl(1)-Cu-Cl(1a)	83.0 (1)	C(1)-N(6)-C(5)	121.9 (2)
Cl(2)-Cu-Cl(1a)	171.3 (1)	N(2)-C(3)-C(4)	123.5 (3)
Cl(3)-Cu-Cl(1a)	91.2 (1)	N(6)-C(5)-C(4)	118.7 (2)
Cu-Cl(1)-Cu(a)	97.0 (1)	C(3)-C(4)-C(5)	117.3 (3)
C(1)-N(2)-C(3)	117.6 (2)		

Table VIII. Thermal Properties

	room temp	phase III	phase II	phase I
$(HAmpym)CuCl_3(H_2O)$				
Single Crystal				
color	green	red	yellow	black
T_{trans}, °C	89	121	220	
ΔH_{trans}, kcal/mol	4.7		4.6	
tot. wt loss, %	5.0	7.3	43.8	
Powder				
color	green	green	dark green	black
T_{trans}, °C	141	~190	~230	
ΔH_{trans}, kcal/mol	2.8		10.1	38.8
tot. wt loss, %	9.3	17.6		45.9

	room temp	phase IV	phase III	phase II
$(H_2Me_2pipz)[CuCl_3(H_2O)]_2$				
Single Crystal				
color	green	red	brown	black
T_{trans}, °C	84	138 (br)	157	210
tot. wt loss, %				43.8
Powder (Fresh)				
color	green	red	brown	black
T_{trans}, °C	83	100	140 (br)	210 (exotherm)
ΔH_{trans}, kcal/mol	3.51 (7)	26.8 (10)	2.4 (2)	

rameters, cation distances and angles, as well as observed and calculated structure factors, have been deposited as supplementary material.

Electronic spectra were recorded on a Perkin-Elmer 330 spectrophotometer. EPR spectra were recorded on a Varian E-3 spectrometer. Magnetic susceptibility data were collected on a PAR vibrating sample magnetometer at Montana State University over the temperature range 4–130 K. IR spectra were recorded on a Perkin-Elmer 283B spectrometer.

Thermal analyses of the two compounds were carried out on either a Mettler TA2000 thermal analyzer or a DSC-2C Perkin-Elmer instrument on both powder and single-crystal samples. Weight loss information was obtained by stopping the thermal scans at selected temperatures and weighing the samples. Visual observation and photographs were made with a Reichert Zetopan optical microscope equipped with interference contrast. A summary of the thermal data obtained is given in Table VIII.

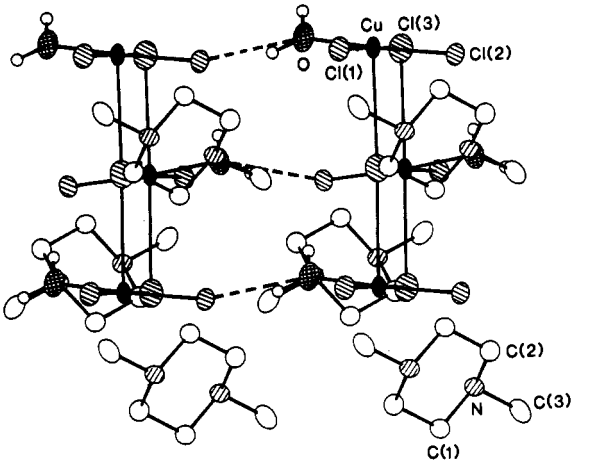

Figure 1. Illustration of the stacks of $CuCl_3(H_2O)^-$ anions in $(H_2Me_2pipz)(CuCl_3(H_2O))_2$. The *b* axis is vertical, and the *a* axis is horizontal. Atoms linked by the interstack hydrogen bonds are denoted by the dashed bonds.

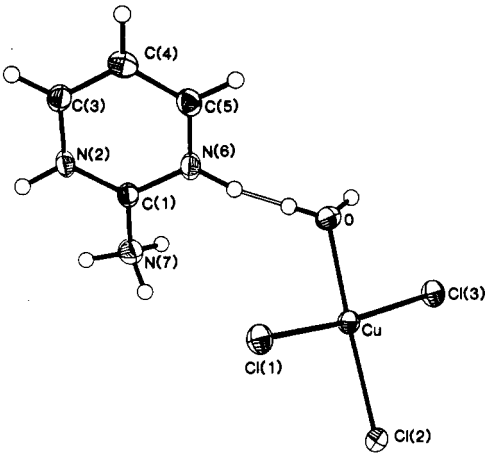

Figure 2. Illustration of the asymmetric unit of $(HAmpym)CuCl_3(H_2O)$, showing the disordered O-H-N(6) hydrogen bond and disordered $-N(7)H_2$ amine group.

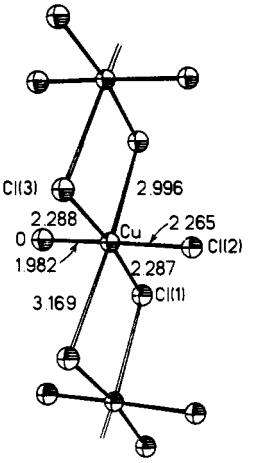

Figure 3. Illustration of the stack of $CuCl_3(H_2O)^-$ anions in the 2-aminopyrimidinium salt. The *a* axis is vertical.

Structure Descriptions

The structures are illustrated in Figures 1–5. The structures of both hydrates consist of stacks of planar $CuCl_3(H_2O)^-$ anions, as seen in Figures 1 and 3. The crystal lattices are stabilized by hydrogen bonding between the water molecules, the counterions,

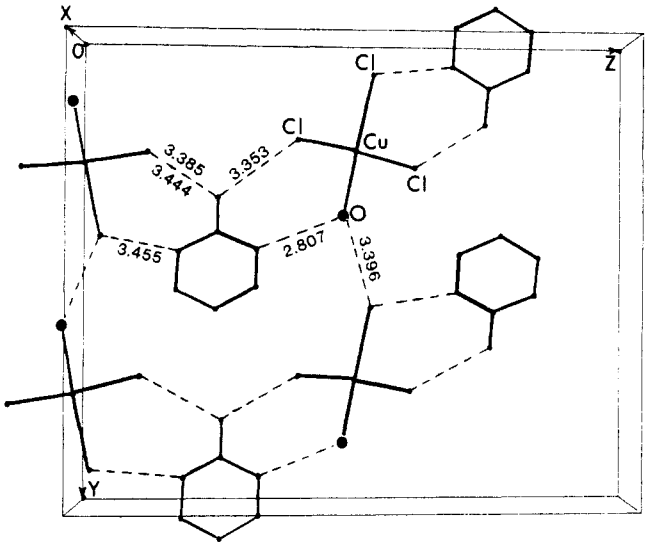

Figure 4. Illustration of the hydrogen-bonding network in (HAmpym)-$CuCl_3(H_2O)$.

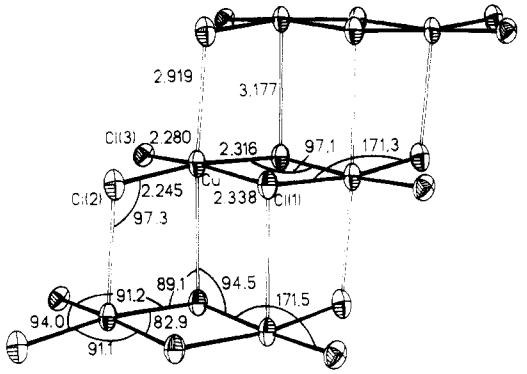

Figure 5. Illustration of the $Cu_2Cl_6^{2-}$ stacks in $(HAmpym)_2Cu_2Cl_6$.

and the halide ions. The planarity of the $CuCl_3(H_2O)^-$ is a consequence of three factors: the small size of the water molecule, which allows the Cl–Cu–Cl angles to open up past 90° without destroying the planarity; the hydrogen bonding to the chloride ions, which reduces their effective charge; and the formation of long semicoordinate bonds to adjacent anions in the stacks. These latter two facts are readily seen in their effect upon the Cu–Cl bond lengths in the dimethylpiperazinium salt where the Cu–Cl(2) (involved in a strong hydrogen bond to the water molecule and the cation) and the Cu–Cl(3) (involved in the semicoordinate bonds) distances are 0.04 Å longer than the Cu–Cl(1) distance. For the 2-aminopyrimidinium salt, all chloride ions are involved in hydrogen bonding, but the bonds to the two chloride ions involved in semicoordinate bond formation, Cl(1) and Cl(3), are 0.02 Å longer than the other Cu–Cl bond.

The stacks are of two different types: simple $1(^1/_2, ^1/_2)$ stacks, IV, in the notation of Geiser et al.,[1c] for the pyrimidinium salt (Figure 4); a more complex $1(^1/_2, ^1/_2, 180°)(-^1/_2, -^1/_2, 180°)$ stack, V, for the piperazinium salt (Figure 1). Adjacent Cu-

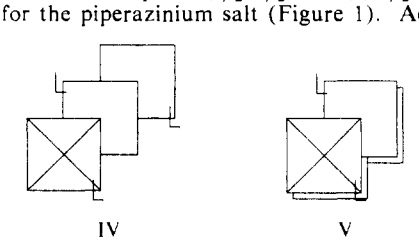

IV V

$Cl_3(H_2O)^-$ groups are related by unit cell translations in the former, and thus all of the $CuCl_3O$ planes in the stacks are parallel. In the latter, adjacent anions are related by a 2_1 operation and hydrogen-bonding interactions (vide infra) cause the $CuCl_3O$ planes to be nonparallel, with a dihedral angle of 11.6° between adjacent planes. In both cases, the stacking leads to the formation of two semicoordinate bonds and a 4 + 2 coordination geometry. The semicoordinate bonds average 3.084 and 3.108 Å, respectively, in the two salts, although in the pyrimidinium salt the two bond lengths are significantly different.

The hydrogen-bonding scheme plays an important role in each structure and is particularly effective in the pyrimidinium salt. In that compound, the hydrogen bonding ties the $[CuCl_3(H_2O)^-]_n$ stacks together into a tight, three-dimensional network (Figure 5). Each 2-aminopyrimidinium anion sits between two adjacent stacks along the *c* axis in such a way that an amino hydrogen and a ring nitrogen are involved in hydrogen bonding to each stack (N–Cl distances from 3.353 to 3.445 Å). The $-NH_2$ group is disordered so as to hydrogen bond to three different chloride ions. Adjacent stacks in the *y* direction (Figure 5) are tied together by O–H···Cl hydrogen bonds (3.396 Å). The ring nitrogen is involved in a disordered (double minimum) N···H···O hydrogen bond (Figure 3) of 2.807 Å length. This corresponds formally to a tautomeric equilibrium of the type pyrimidine–water ↔ pyrimidinium–hydroxide. This would indicate that the basicity of the monoprotonated pyrimidinium ring is rather low. In the piperazinium salt, O–H···Cl(2) bonds hold adjacent stacks together in the *x* direction, while along the *c* axis, Cl···H–$N(C_2H_4)_2$N–H···Cl linkages provide stability. The second water proton is involved in an intrastack hydrogen bond, causing the adjacent $CuCl_3O$ planes to tilt with respect to each other.

This is the first time that the planar $CuCl_3(H_2O)^-$ species has been reported in solid-state copper(II) halide chemistry and as such provides a novel intermediate between the planar $CuCl_2(H_2O)_2$ species and $CuCl_4^{2-}$ species. The existence of the monohydrate has been proposed in solution.[14] Its existence also ties in with the recently reported planar $Cu_2Cl_5(H_2O)^-$ dimers,[10] where again extensive hydrogen bonding and stacking contribute to their stability, and with the planar $Cu_3Cl_7(HOEt)^-$ trimer.[15] Thus, perhaps the $Cu_3Cl_6(H_2O)_2$ and $Cu_5Cl_{10}(C_3H_7OH)_2$ oligomers[16] are not as unusual as initially thought.

The crystal structure of the anhydrous pyrimidinium salt contains stacks of planar, symmetrically bibridged $Cu_2Cl_6^{2-}$ dimers, as illustrated in Figure 5. Within the dimers, the bridging Cu–Cl distances are substantially longer (2.316 (1), 2.338 (1) Å) than the terminal Cu–Cl distances (2.245 (1), 2.280 (1) Å). This is in accord with the general trend observed in $Cu_nCl_{2n+2}^{2-}$ oligomers.[17] The shorter terminal Cu–Cl distance is to the chlorine atom not involved in N–H···Cl hydrogen bonding. The stacking is a generalization to dimeric species of the type I stacking pattern, denoted by $2(^1/_2, ^1/_2)$ in the notation of ref 1c. The semicoordinate distance between adjacent dimers are 2.996 (1) and 3.169 (1) Å. The hydrogen bonding may be described as follows: The ring N–H group hydrogen bonds to a terminal chloride ion (Cl(3); N···Cl = 3.291 Å), the two disordered amino N–H groups hydrogen bond to the bridging chloride ion (Cl(1); N···Cl = 3.319 Å) and to a terminal chloride on an adjacent dimer in the stack (Cl(3); N···Cl(3); N···Cl = 3.291 Å), and finally, the ordered N–H group hydrogen bonds to a ring nitrogen on a centrosymmetrically related cation (N(2); N···N = 2.957 Å). The structure thus consists of the $(Cu_2Cl_6^{2-})_n$ stacks, separated by, and hydrogen bonded to, 2-aminopyrimidinium dimers.

Thermal Analysis

The thermal properties of these hydrated compounds are interesting because of the contrasting behavior recorded for powders and single crystals during the initial dehydration. This is particularly true for the pyrimidinium salt. The powdered samples lose water smoothly up to 140 °C, while single crystal fragments show the presence of two peaks near 100 °C, the second of which appears to originate in a very sharp manner. To further char-

(14) Ramette, R.; Fan, G. *Inorg. Chem.* **1983**, *22*, 3323.
(15) Grigereit, T. E.; Ramakrishna, B. L.; Place, H.; Willett, R. D.; Pellacani, G. C.; Manfridini, T.; Menabue, L.; Bonamartini-Corradi, A.; Battaglia, L. P. *Inorg. Chem.* **1987**, *26*, 2235.
(16) Willett, R. D.; Rundle, R. E. *J. Chem. Phys.* **1964**, *40*, 838.
(17) Willett, R. D. *Acta Crystallogr., Sect. B* **1988**, *B44*, 503.

acterize this behavior, optical microscopy investigations were undertaken. Two phenomena were observed for single crystals in the range of temperatures where the thermal peaks were found: a reorganization of the surface following the dehydration in the temperature range 60–100 °C and a sudden formation of a liquid phase, which burst from the crystal and underwent immediate crystallization at 120 °C. A similar behavior has been observed in the dehydration of tetragonal nickel sulfate hexahydrate[18a,b] and was attributed to the formation of a poorly permeable surface layer hindering the free escape of the gaseous reaction product. Photoacoustic evidence about the formation of the above layer has also been obtained.[18c] Furthermore, a surface dehydrated layer appears to be of paramount importance in water loss from the sodium thiosulfate pentahydrate cleavage surfaces.[19]

In contrast with the behavior in dehydration, the final decomposition/melting endotherm is smooth for crystals and structured for powders. The latter structure changes shape remarkably, however, if a lid, which prevents the free escape of the decomposition product, is placed on the otherwise open sample pan. This suggests that the observed structure might be the result of decomposition/reaction or desorption/adsorption cycles made by the volatile product during its way out through the particulate material. White NH_4Cl sublimate is observed to form on the cool walls of the thermal apparatus, and dark brown patches form and grow on the surface of the microscopically observed crystals.

On the basis of the above data, the following observations and conjectures about the physical processes involved in the transformations can be given:

(a) Extended dehydration patches observed on the surfaces of exposed single crystals indicate that water loss can take place at room temperature. The remaining water molecules then escape almost freely through the damaged surface as the temperature is raised.

(b) In contrast, the initial dehydration process in fresh crystals generates an almost impermeable layer on the less damaged single-crystal surfaces (first peak), which prevents the further escape of the solvent. This induces the dissolution of the material in its own solvent and produces a liquid phase. At slightly higher temperatures, the superheating of this solution overcomes the resistance of the surface layer and it is expelled violently from the crystal (second sharp peak).

(c) It is significant that the dehydration patches have a shape strongly elongated in a direction parallel to that of the chains within the crystal. In contrast, when ammonium chloride is lost and dark brown patches form after the 140 °C transition in the powder, these appear round and grow radially. Thus, the dehydration process in the crystal is structure sensitive, while the decomposition has the aspect of an "isotropic" transformation taking place in a polycrystalline material residue of preceding transformations.

A comparison of the thermal behavior described above for the pyrimidinium compound with the closely related piperazinium one shows both analogies and dissimilarities. For the latter compound, the dehydration has been found to be strongly dependent on the aging of the material. A low-temperature (ca. 70–80 °C) dehydration peak, found with fresh samples, is absent in aged materials. The second broad dehydration endotherm is also observed to change shape. The above features can be again related to surface layer sensitive water loss. In addition, microscopy indicates that "nucleation" on the crystal surfaces does not show any preferential directioning. This might be due to the alternating disposition of the water molecules along the chains, since channels parallel to the chain axis cannot be formed.

For both aged and fresh materials, a phase transition is recorded at ca. 140 °C, before the end of the dehydration. This suggests that the dehydration product reorganizes into a lower hydrate before completing the dehydration process. At variance with the pyrimidinium salt, an increase in temperature leads to a rather broad but small exotherm for the piperazinium cuprate. This is perhaps due to a slow crystallization of amorphous material formed during the dehydration. Endothermal loss of a volatile material then takes place, coupled with melting. However, this time it is followed by a large final exotherm, which is due to both decomposition in the liquid phase and crystallization of a reddish product from the decomposed melt.

Structurally it is quite easy to visualize a possible sequence of events that occurs upon dehydration of single crystals of $(C_4N_3H_6)CuCl_3(H_2O)$. The structure consists of identical layers, as illustrated in Figure 5. Layers are linked by semicoordinate Cu···Cl bonds, yielding asymmetric bibridged chains parallel to the needle axis (Figure 4). At the first transition temperature, the copper–water bonds break and the water molecules are free to move through the channels thus formed. Simultaneously, the asymmetric bridges in the chain could transform into symmetric bridges. A similar mechanism has been proposed for the dehydration of $CuCl_2 \cdot 2H_2O$.[20] This would yield five-coordinate (square-pyramidal) symmetrically bibridged chains. These structures are known to have a red color. Note that the apical bonds are all cis—e.g.—on the same side of the chain, an energetically and structurally unfavorable situation. The water molecules, although free to move, are still constrained to the channels and block both the coordination of the cation to the chain and the coupling of neighboring $CuCl_3^-$ groups to form the $Cu_2Cl_6^{2-}$ dimer units found in single crystals of the anhydrous material. In rapid heating runs, they cannot diffuse rapidly enough to reach and diffuse through the ends of the crystals (the 001 and $00\bar{1}$ faces). At the second transition temperature (T = 121 °C), the water has become superheated and is forcefully ejected from the crystals. This clears the channels, and the monoprotonated cations are able to coordinate to the copper ion to yield the yellow high-temperature structure, which we postulate to contain planar $CuCl_3(pyrimidinium)^-$ units, in which the unprotonated ring nitrogen atom coordinates to the Cu(II) ion.

Spectroscopy and Magnetism

The electronic absorption spectrum at room temperature for the pyrimidinium and piperazinium salts consists of an intense broad unresolved band in the d–d region, centered at 12 500 cm^{-1}, and of a series of charge-transfer bands in the UV region at 27 000, 33 000, and 39 000 cm^{-1}. The first band, which contains in its envelope the three expected d–d transitions, agree very well with the spectra observed for elongated octahedral coordination in Cu(II) salts. In particular, as seen in Table IX, a smooth decrease in band maximum occurs as Cl^- is replaced by H_2O as a ligand. While apparently contradictory to behavior predicted by crystal field effects, the shift is probably dictated by changes in the axial coordination.

The charge-transfer spectra show more interesting features. Three bands are present in both compounds at ~27 000, 33 000, and 38 000 cm^{-1}. These are usually assumed to be due to transitions between the low-lying bonding (or nonbonding) ligand orbitals and the half-occupied $d_{x^2-y^2}$-like orbital. In particular the first charge-transfer bands of the $(RNH_3)_2CuCl_4$ and $ACuCl_3(H_2O)$ compounds, which occur at 24 000 and 27 000 cm^{-1}, respectively (Table IX), may be assigned to transitions arising from the halide nonbonding π orbitals. These are absent in the $CuCl_2(H_2O)_2$ system, and thus, the first ligand → metal charge-transfer bands lie at substantially higher energies. The bands at frequencies greater than 30 000 cm^{-1} can be assigned to transitions arising from π-bonding molecular orbitals.

The IR spectrum of the *N,N'*-dimethylpiperazinium hydrochloride salt in the low-energy region (350–60 cm^{-1}) contains a very strong and broad band, centered at about 200 cm^{-1}, which, on the basis of shape and position, is assignable to the strong

(18) (a) Guarini, G. G. T.; Rustici, M. *React. Solids* **1987**, *2*, 381. (b) Guarini, G. G. T.; Rustici, M. *J. Therm. Anal.* **1988**, *34*, 481. (c) Guarini, G. G. T.; Magnani, A. *React. Solids*, in press.
(19) Guarini, G. G. T.; Piccini, S. *J. Chem. Soc., Faraday Trans. I* **1988**, *84*, 331.
(20) Engberg, A. *Acta Chem. Scand.* **1970**, *24*, 3510.
(21) Correa de Mello, P.; Hehenberger, M.; Larsson, S.; Zerner, M. *J. Am. Chem. Soc.* **1980**, *102*, 1278.

Table IX. Spectral Parameters for Planar Copper(II) Chloride Complexes

	complex (coordn)			
	$CuCl_4^{2-}$ [a] (isolated)	$CuCl_4^{2-}$ [b] (4 + 2)	$CuCl_3(H_2O)^-$ [c] (4 + 2)	$CuCl_2(H_2O)_2$ [d] (4 + 2)
d–d band (max), cm^{-1}	16000	12800	12500	12100
first CT band, cm^{-1}	26000	24000	27000	36000
$g_\parallel$	2.21	2.27	2.30	2.352
$g_\perp$	2.05	2.05	2.06	2.080, 2.037
IR bands, cm^{-1}	276, 285, 314	278, 294	265–275, 310–320	242, 289

[a] Antolini, L.; Benedetti, A.; Fabretti, A. C.; Giusti, A. *Inorg. Chem.* **1988**, *27*, 2192. McDonald, R. G.; Hitchman, M. A. *Inorg. Chem.* **1986**, *258* 3273. Harlow, R. L.; Wells, W. J.; Watt, G. W.; Simonsen, S. H. *Inorg. Chem.* **1975**, *14*, 1768. [b] For $(RNH_3)_2CuCl_4$ layer perovskites: Abdalaziz, D.; Thrierr-Sorel, A.; Perret, R.; Chaillot, B.; Guerchaio, J. E. *Bull. Soc. Chim. Fr.* **1975**, *3–4*, 535. Wong, R. J. H.; Willett, R. D.; Drumheller, J. E. *J. Chem. Phys.* **1981**, *74*, 6018. Willett, R. D.; Ferraro, J. R.; Choco, M. *Inorg. Chem.* **1974**, *13*, 2919. [c] This work. [d] Andreev, S. N.; Sapozhnikova, O. V. *Russ. J. Inorg. Chem. (Engl. Transl.)* **1965**, *10*, 1379. Pake, G. E. *Paramagnetic Resonance*; W. A. Benjamin Inc.: New York, 1962; p 192. Howell, R. A.; Keeton, D. P. *Spectchim. Acta* **1966**, *22*, 1211. Adams, D. M.; Lock, P. J. *J. Chem. Soc. A* **1967**, 620.

hydrogen-bonding interactions among chlorine anions and organic cations, as well as several other lattice vibrations at lower frequencies. In the same spectral region the copper(II) complex presents new bands, centered at 359 ms, 310 vs, 276 s, and 239 m cm^{-1}. The IR spectrum of the hydrated pyrimidinium salt in the low-energy region shows a weak, broad band at 265–275 cm^{-1} and a strong broad band at 320 cm^{-1}. The bands in the 310–320-cm^{-1} and 265–275-cm^{-1} range can be tentatively assigned to the two predicted trans equatorial Cu–Cl vibrations and to the expected vibration of the Cu–Cl linkage trans to the coordinated water molecule. The 359-cm^{-1} band in the dimethylpiperazinium salt disappears upon dehydration, so it can be assigned as a Cu–O mode.

The magnetic data for both compounds showed small antiferromagnetic deviation from Curie behavior. The data for the 2-aminopyrimidinium salt was fit to a 1D linear-chain model[22] with a mean field correction for interchain coupling introduced via the relation $\chi_{MF} = \chi_{1D}T/(T + \theta)$. The least-squares results, with the exchange parameter defined by

$$\mathcal{H} = -2J\sum_i \vec{S}_i\cdot\vec{S}_{i+1}$$

gave J/k = 3.1 (1) K, g = 2.119 (3), and θ = 0.2 (1) K (Figure 6). Because of some irreproducibility in the higher temperature data, no attempt was made to fit the high-temperature data to the model. The data for the *N,N'*-dimethylpiperazinium complex exhibited only a small antiferromagnetic coupling, as evidenced by a smaller deviation from linearity on a $\chi_m T$ vs T plot.

Structurally, it is reasonable to assume that the antiferromagnetic intrachain coupling occurs via the Cu···Cl bridges in the $[CuCl_3(H_2O)]^-$ chains. However, the presence of a significant interchain pathway in the pyrimidinium salt (see Figure 4) involving a Cu–O–H···Cl–Cu linkage is to be noted. Such interactions can be relatively significant and are usually of a ferromagnetic nature.[23] Thus, the observed ferromagnetic value of θ = 0.2 K may be due to these interchain hydrogen bonds.

The room-temperature powder EPR spectrum of both salts shows a typical axial pattern with $g_\perp \sim 2.08$ and $g_\parallel \sim 2.30$. However, in each case, the perpendicular feature is broad and shows evidence at liquid-nitrogen temperature of the presence of two components. This is consistent with the structural features. Single-crystal EPR of the 2-aminopyrimidinium salt yielded g_a = 2.304, g_b = 2.174, and g_c = 2.060. Angular dependent spectra in both the *ab* and *bc** planes show asymmetric absorption lines, indicating the presence of unresolved, overlapping lines. Thus, the two magnetically inequivalent sites, which are separated by the pyridinium cations, are not strongly coupled and an upper limit of an effective field of 200 Oe (0.02 cm^{-1}) can be placed on this intersite coupling. Detailed analysis of the line shape of the overlapping spectra at one orientation[24] yielded $|J'/k|$ = 0.0007 cm^{-1}.

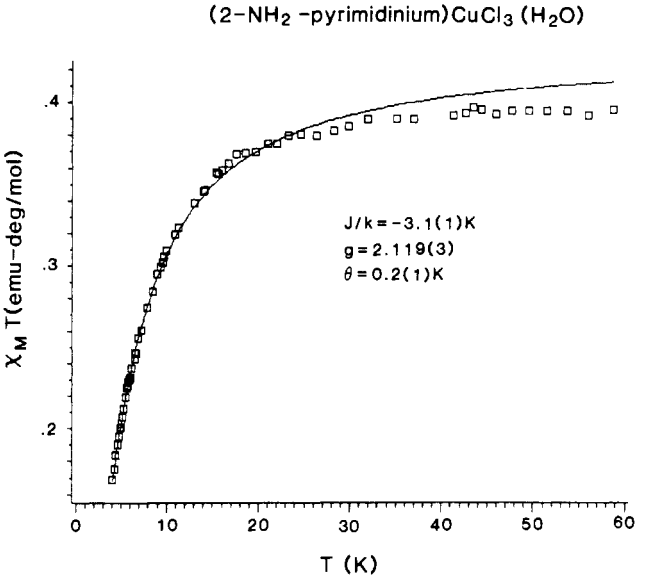

Figure 6. Plot of $\chi_m T$ versus T for (HAmpym)$CuCl_3(H_2O)$.

Crystal Chemistry

The past decade has seen a veritable explosion in the number of crystal structures of copper(II) halide complexes that have been determined. This has included the structures of large numbers of CuX_2L_2 and CuX_2L^2 complexes (X = halide, L = monodentate ligand, L^2 = bidentate ligand). Three general structural types can be reorganized: isolated four-coordinate species with distorted tetrahedral coordination geometry;[25a] dimerized species with two bridging halide ions yielding a square-pyramidal or folded 4 + 1 coordination geometry;[25b] stacked, planar species with a tetragonally elongated 4 + 2 coordination geometry. As these have appeared, it has been possible to observe and deduce certain structural characteristics. The correlation of physical properties, such as the electronic absorption spectra[26a] or the magnetic behavior,[26b] with variations in structural parameters has been a subject of considerable importance. However, since structures frequently are reported as adjuncts to other studies, their significance for these investigations may not be recognized. In Appendix A (supplementary material), we have brought together

(22) Baker, G. A., Jr.; Gilbert, H. E.; Eve, J.; Rushbrook, G. S. *Phys. Lett.* **1967**, *25A*, 207.
(23) Groenendijk, H. A.; Blote, H. W. J.; van Duyneveldt, A. J.; Gaura, R. M.; Landee, C. P.; Willett, R. D. *Physica* **1981**, *106B*, 47.
(24) Hoffmann, S. K. *Chem. Phys. Lett.* **1983**, *98*, 329.
(25) (a) Cingi, M. B.; Lanfredi, A. M. M.; Tiripicchio, A. *Acta Crystallogr., Sect. C* **1987**, *C43*, 834. (b) Hoffmann, S. K.; Towle, D. K.; Hatfield, W. E.; Weighardt, K.; Chaudhuri, P.; Weiss, J. *Mol. Cryst. Liq. Cryst.* **1984**, *107*, 161. Marsh, W. E.; Hatfield, W. E.; Hodgson, D. J. *Inorg. Chem.* **1988**, *27*, 1819. Rojo, T.; Arriortua, M. E.; Ruiz, J.; Darriet, J.; Villeneuve, G.; Baltan-Porter, D. *J. Chem. Soc., Dalton Trans.* **1987**, 285.
(26) (a) Desjardines, S. R.; Wilcox, D. E.; Musselman, R. L.; Solomon, E. T. *Inorg. Chem.* **1987**, *26*, 288. Charlot, M.-F.; Journaux, Y.; Kahn, O.; Bencini, A.; Gatteschi, D.; Zanchini, C. *Inorg. Chem.* **1986**, *25*, 1060. (b) *Magneto-Structural Correlations in Exchange Coupled Systems*; Willett, R. D., Gatteschi, D., Kahn, O., Eds.;, D. Reidel, publishers, NATO ASI Series; D. Reidel: Dordrecht, The Netherlands, 1985; Vol. 140.

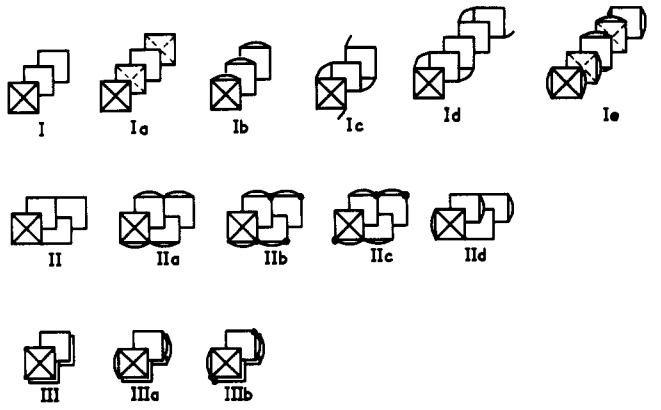

Figure 7. Stacking patterns for planar CuX_2L_2 and CuX_2L^2 species. L = monodentate; L^2 = bidentate ligand. The L^2 ligands are denoted by the curved lines; asymmetric bidentate ligands are denoted by the dotted curved lines. See Table 11s (Appendix A) (supplementary material) for a listing of compounds exhibiting these patterns.

a compilation of all planar, monomeric CuX_2L_2 and CuX_2L^2 compounds in which aggregation of the monomers occurs with the formation of stacks similar to those reported for the $CuCl_3(H_2O)^-$ reported in this paper. Similar compilations of crystallographic and structural data have been given for $ACuCl_3$ salts,[1b] stacked planar oligomers with $n \geq 2$,[1c,10b] A_2CuX_4 layered perovskite structures,[27a] and isolated $Cu_2X_6^{2-}$ species,[27b] as well as a rather incomplete listing of the structures containing isolated $CuCl_4^{2-}$ anions.[28]

Stacking of planar CuL_4 species, so as to complete the 4 + 2 coordination for each copper ion, yields asymmetric bibridged chains. Three basic stacking patterns are observed: $1(^1/_2, ^1/_2)$, $1(^1/_2, ^1/_2)(^1/_2, -^1/_2)$, and $1(^1/_2, ^1/_2)(-^1/_2, -^1/_2)$, shown in I–III, respectively. Subtle variations occur in each of these, depending upon the nature of the ligands. The distribution of known structures among patterns I–III are 17, 8, 12 (X = Cl) and 5,2, 3 (X = Br), respectively, as well as one type II X = F salt.[72] For monodentate ligands forming *trans*-CuX_2L_2 complexes, type I stacking almost invariably occurs.[29,33,34,40,41,43,47,49,50,52,54,58,60,61,65,69] With CuX_3L species, either type I or III stacks are found.[31] With bidentate ligands, *cis*-CuX_2L^2 complexes are formed. Steric forces then favor type II or type III stacks. The various compounds adopting these stacked structures,[29–72] with major structural parameters, are given in Table 11s of Appendix A (supplementary Material).

The crystal chemistry becomes exceptionally rich when the bidentate nature of the L^2 ligands is included in the stacking diagrams, as seen in Figure 7. For type I stacks, only the Ib pattern is observed,[39] and it clearly will be energetically favorable only when L^2 is a flat, planar ligand. Type IIa stacks[35,53,63] and IIIa stacks[31,38,44,45,46,55] can be adopted by bulkier ligands. The unusual IId pattern[57] has the same steric restrictions on the nature of L^2 as the Ib pattern. When the L^2 ligand is stereochemically asymmetric, additional freedom is introduced. Thus, the IIb and IIc patterns are adopted by the two different crystal forms of $CuCl_2(NH_2NHCONH_2)_2$.[42] With the type III patterns, only the IIIb stacking variation has been found.[30,32,36,51,56,67] An interesting variation occurs for the type I stacks when the bidentate ligand bridges adjacent CuL^4 chromophores, as illustrated in Ic.[48,59] This bridging capability becomes incorporated in a highly unusual way in the $Cu_3Cl_8(adeninium)_2 \cdot 4H_2O$ salt, which can be described as a stack of stacked trimers (Id).[37]

In summary, the stacking diagrams illustrated in Figure 7 provide a convenient mechanism to classify the asymmetrically bibridged chains on planar CuX_2L_2 and CuX_2L^2 salts and the usefulness of these simple stacking diagrams to summarize the structural relationships is clearly seen. The major features of the more than 40 observed structures are embodied in the three major classifications, I–III. Finer details and perturbations are revealed in the further subclassifications. The uniform type stacking, I, is most commonly observed, while the "stair"-like stacks, II, are the rarest. The "ladder" type stacks, III, have been of special interest magnetically because of possible next-nearest-neighbor

(27) (a) Willett, R. D.; Place, H.; Middleton, M. *J. Am. Chem. Soc.* **1988**, *110*, 8639. (b) Landee, C. P.; Djili, A.; Mudgett, D. F.; Newhall, M.; Place, H.; Scott, B.; Willett, R. D. *Inorg. Chem.* **1988**, *27*, 620.
(28) Noren, B.; Oskarsson, A.; Svensson, C.; Soto, L.; Ruiz, J.; Colacio, E. *Acta Chem. Scand.* **1989**, *43*, 368.
(29) Aliev, N. A.; Abdullaev, G. K.; Aliev, R. Y. A.; Guseinov, N. M.; Kuliev, A. D. *Russ. J. Inorg. Chem. (Engl. Transl.)* **1973**, *18*, 443.
(30) Bream, R. A.; Estes, E. D.; Hodgson, D. J. *Inorg. Chem.* **1975**, *14*, 1672.
(31) Brown, D. B.; Donner, J. A.; Hall, J. W.; Wilson, S. R.; Wilson, R. B.; Hodgson, D. J.; Hatfield, W. E. *Inorg. Chem.* **1979**, *18*, 2635.
(32) Bukovec, P.; Golic, L.; Orel, B.; Kobe, J. *J. Carbohydr., Nucleosides, Nucleotides* **1981**, *8*, 1.
(33) Bukowska-Strzyzewska, M.; Skoweranda, J. *Acta Crystallogr., Sect. C* **1987**, *C43*, 2290.
(34) Cartwright, B. A.; Goodgame, M.; Johns, K. W.; Skapski, A. C. *Biochem. J.* **1978**, *175*, 337.
(35) Churchill, M. R.; Hutchinson, J. P. *Cyrst. Struct. Commun.* **1980**, *9*, 1209.
(36) Colyvas, K.; Tietze, H. R.; Egri, S. K. J. *Aust. J. Chem.* **1982**, *35*, 1581.
(37) De Meester, P.; Skapski, A. C. *J. Chem. Soc., Dalton Trans.* **1972**, 2400.
(38) Endres, H. *Acta Crystallogr., Sect. C* **1983**, *C39*, 1192.
(39) Endres, H.; Genc, N.; Nothe, D. *Z. Naturforsch.* **1983**, *38B*, 90.
(40) Engberg, A. *Acta Chem. Scand.* **1970**, *24*, 3510.
(41) Estes, W. E.; Gavel, D. P.; Hatfield, W. E.; Hodgson, D. J. *Inorg. Chem.* **1978**, *17*, 1415.
(42) Villa, A. C.; Manfredoti, A. G.; Nardelli, M.; Pelizzi, G. *J. Cryst. Mol. Struct.* **1971**, *1*, 245–251.
(43) Galkin, A. A.; Ivanova, S. V.; Kamenev, V. I.; Polyakov, P. I. *Sov. Phys. Solid State* **1979**, *21*, 1486.
(44) Giacovazzo, C.; Scandale, E.; Scordari, F. *Z. Kristallogr.* **1976**, *144*, 226.
(45) Harvey, D. A.; Lock, C. J. L. *Acta Crystallogr., Sect. C* **1986**, *C42*, 799.
(46) Helis, H. M.; Goodman, W. H.; Wilson, R. B.; Morgan, J. A.; Hodgson, D. J. *Inorg. Chem.* **1977**, *16*, 2412.
(47) Jansen, J. C.; von Koningsveld, H.; van Ooijen, J. A. C. *Cryst. Struct. Commun.* **1978**, *7*, 637.
(48) Jarvis, J. A. J. *Acta Crystallogr.* **1962**, *15*, 964.
(49) Laing, M.; Carr, G. *J. Chem. Soc. A* **1971**, 1141.
(50) Laing, M.; Horsfield, E. *Chem. Commun.* **1968**, 735.
(51) Lundberg, B. K. S. *Acta Chem. Scand.* **1972**, *26*, 3977.
(52) Marsh, W. E.; Valente, E. J.; Hodgson, D. J. *Inorg. Chim. Acta* **1981**, *51*, 49.
(53) Megnamisi-Belombe, M.; Singh, P.; Bolster, D. E.; Hatfield, W. E. *Inorg. Chem.* **1984**, *23*, 2578.
(54) Moroson, B. *Acta Crystallogr., Sect. B* **1975**, *B31*, 632.
(55) O'Connor, C. J.; Eduok, E. E.; Fronczek, F. R.; Kahn, O. *Inorg. Chim. Acta* **1985**, *105*, 107.
(56) Ohsawa, A.; Akimoto, T.; Tsuji, A.; Igeta, H.; Iitaka, Y. *Tetrahedron Lett.* **1978**, *23*, 1979.
(57) Olmstead, M. M.; Musker, W. K.; Ter Haar, L. W.; Hatfield, W. E. *J. Am. Chem. Soc.* **1982**, *104*, 6627.
(58) Pabst, I.; Bats, J. W. *Acta Crystallogr., Sect. C* **1985**, *C41*, 1297.
(59) Papavinasam, E.; Natarajan, S. *Z. Kristallogr.* **1985**, *172*, 251.
(60) Peterson, S. W.; Levy, H. *J. Chem. Phys.* **1957**, *26*, 220.
(61) Serator, M.; Langfelderova, H.; Gazo, J.; Stracelsky, J. *Inorg. Chim. Acta* **1978**, *30*, 267.
(62) Sheldrick, W. S.; Bell, P. *Z. Naturforsch.* **1987**, *42B*, 195.
(63) Sillanpaa, R. *Inorg. Chim. Acta* **1984**, *82*, 75.
(64) Van de Leemput, P. J. H. A. M.; Cras, J. A.; Willemse, J.; Beurskens, P. T.; Menger, E. *Recl. Trav. Chim. Pays-Bas* **1976**, *95*, 191.
(65) Van Ooijen, J. A. C.; Reedijk, J. *Transition Met. Chem.* **1979**, *4*, 305.
(66) Van Ooijen, J. A. C.; Reedijk, J. *Inorg. Chim. Acta* **1977**, *25*, 131.
(67) Rojo, T.; Mesa, J. L.; Arriortua, M. I.; Savariault, J. M.; Galy, J.; Villeneuve, G.; Beltran, D. *Inorg. Chem.* **1988**, *27*, 3904.
(68) Cartwright, B. A.; Goodgame, M.; Johns, K. W.; Skapski, A. C. *Biochem. J.* **1978**, *175*, 337.
(69) Pon, G.; Willett, R. D. *Acta Crystllogr.*, manuscript in preparation.
(70) Garland, M. T.; Grandjean, D.; Spodine, A.; Atria, A. M.; Manzur, J. *Acta Crystallogr., Sect. C* **1988**, *C44*, 1209.
(71) Garland, M. T.; Grandjean, D.; Spodine, A.; Atria, A. M.; Manzur, J. *Acta Crystallogr., Sect. C* **1988**, *C44*, 1547.
(72) Oosterling, A. J.; deGraaff, R. A. G.; Haasnoot, J. G.; Keij, F. S.; Reedijk, J.; Pedersen, E. *Inorg. Chim. Acta* **1989**, *163*, 53.

interactions along the chains. The number of bromide complexes that have been studied is significantly smaller than the number of chlorides. From magnetic interests, this is unfortunate, since exchange couplings are typically larger for copper(II) bromide complexes.

Acknowledgment. The support of NSF Grant DMR 8803382 is acknowledged. The WSU X-ray diffraction laboratory was established through funds from NSF Grant CHE-8408407 and The Boeing Corp.

Supplementary Material Available: Listings of hydrogen positional coordinates, anisotropic thermal parameters, and bond distances and angles for $(HAmpym)CuCl_3(H_2O)$ (Table 1s) and $(H_2Me_2pipz)[CuCl_3(H_2O)]_2$ (Tables 3s-5s), hydrogen positional coordinates and anisotropic thermal parameters for $(HAmpym)_2Cu_2Cl_6$ (Tables 7s and 8s), and data collection and refinement parameters (Table 10s), a packing diagram for $(HAmpym)_2Cu_2Cl_6$, and Appendix A, containing text discussing stacked copper complexes and a listing of structural parameters for stacked copper species (Table 11s) (22 pages); listings of observed and calculated structure factors (Tables 2s, 6s, and 9s) (38 pages). Ordering information is given on any current masthead page.

Contribution from the Chemistry Department, D-006, University of California at San Diego, La Jolla, California 92093, and Department of Chemistry, University of Delaware, Newark, Delaware 19716

Trialkoxysiloxy Complexes of Nickel. Molecular Structures of $Na_3(\mu_3\text{-}I)\{Ni[\mu_3\text{-}OSi(O^tBu)_3]_3I\}\cdot 0.5THF\cdot 0.5C_5H_{12}$ and $\{(\eta^3\text{-}C_3H_5)Ni[\mu_2\text{-}OSi(O^tBu)_3]\}_2$

Anne K. McMullen,† T. Don Tilley,*,† Arnold L. Rheingold,*,‡ and Steven J. Geib‡

Received September 25, 1989

The nickel siloxide complex $Na_3(\mu_3\text{-}I)\{Ni[\mu_3\text{-}OSi(O^tBu)_3]_3I\}\cdot 0.5THF\cdot 0.5C_5H_{12}$ (**1**) is prepared by reaction of $NiI_2(THF)_2$ with $NaOSi(O^tBu)_3$ in refluxing tetrahydrofuran. The dimeric allyl derivative $\{(\eta^3\text{-}C_3H_5)Ni[\mu_2\text{-}OSi(O^tBu)_3]\}_2$ (**2**) is obtained from $Ni(\eta^3\text{-}C_3H_5)_2$ and $HOSi(O^tBu)_3$. Complex **1** crystallizes in space group $P\bar{1}$ with a = 13.953 (2) Å, b = 14.042 (2) Å, c = 18.934 (3) Å, α = 80.61 (1)°, β = 87.27 (1)°, γ = 60.02 (1)°, V = 3168 (1) Å^3, Z = 2, and R_F = 4.65%. Complex **2** crystallizes in space group $P2_1$ with a = 14.474 (4) Å, b = 10.336 (2) Å, c = 15.651 (3) Å, β = 117.42 (2)°, V = 2078.2 (8) Å^3, Z = 4, and R_F = 6.20%.

There is renewed interest in alkoxy and siloxy complexes of the transition metals, partly because such species are being shown to display unusual and interesting reactivity patterns.[1] Also, these compounds are becoming popular as precursors to oxide ceramic materials.[2] Trialkoxysiloxy ligands, $-OSi(OR)_3$,[3-6] can potentially provide unique electronic and structural properties for transition-metal derivatives. For example, the presence of four donor atoms creates the possibility for these ligands to behave in a multidentate fashion. We are therefore interested in exploring the coordination chemistry of such ligands and in delineating structural and chemical properties that result from their coordination to transition metals. One goal of this work is to develop complexes that may function as convenient molecular precursors to transition-metal oxide and silicate materials via hydrolysis or thermolysis.

The chemistry of nickel alkoxides has not been extensively developed,[1f,g] and to our knowledge the only previous reports of siloxide derivatives describe $[(PMe_3)(Me)Ni(\mu_2\text{-}OSiMe_3)]_2$[7] and $PhSi(OH)_2ONiOSi(OH)PhOSi(OH)_2Ph$,[8] although polymeric species with Ni–O–Si linkages have been prepared.[9] In this paper, we describe the synthesis and characterization of two tri-*tert*-butoxysiloxy derivatives of nickel, $Na_3(\mu_3\text{-}I)\{Ni[\mu_3\text{-}OSi(O^tBu)_3]_3I\}\cdot 0.5THF\cdot 0.5C_5H_{12}$ (**1**) and $\{(\eta^3\text{-}C_3H_5)Ni[\mu_2\text{-}OSi(O^tBu)_3]\}_2$ (**2**).

Results and Discussion

Anhydrous nickel halides $NiCl_2$ and $NiBr_2$ are unreactive toward either $NaOSi(O^tBu)_3$ or $LiOSi(O^tBu)_3$ in diethyl ether or dichloromethane, presumably because of the insolubility of the metal dihalide. However, $NiI_2(THF)_2$ reacts slowly with $NaOSi(O^tBu)_3$ in refluxing tetrahydrofuran to form a nickel siloxide complex that crystallizes from pentane as the blue solvate $Na_3(\mu_3\text{-}I)\{Ni[\mu_3\text{-}OSi(O^tBu)_3]_3I\}\cdot 0.5THF\cdot 0.5C_5H_{12}$ (**1**, eq 1).

Crystals of this compound decompose slowly over a few months when stored under nitrogen at room temperature. Once isolated, compound **1** decomposes when redissolved in pentane, diethyl ether, benzene, or dichloromethane, as evidenced by rapid discoloration of the solution and precipitation of NaI. The compound is more stable in tetrahydrofuran, and recrystallization from pentane is possible in the presence of a small amount of tetrahydrofuran. The room-temperature EPR spectrum of a powdered

$$NiI_2(THF)_2 + 2\,NaOSi(O^tBu)_3 \xrightarrow[\text{reflux}]{\text{THF}} \quad (1)$$

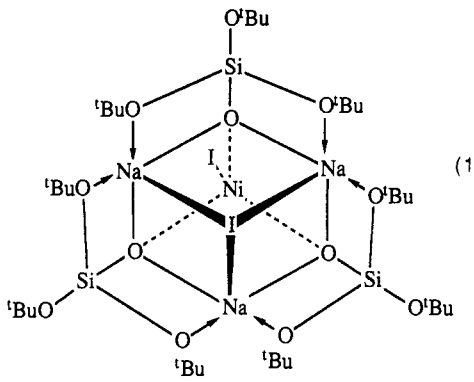

1

† University of California at San Diego.
‡ University of Delaware.

(1) For example: (a) Power, P. P. *Comments Inorg. Chem.* **1989**, *8*, 177. (b) Rothwell, I. P. *Acc. Chem. Res.* **1988**, *21*, 153. (c) LaPointe, R. E.; Wolczanski, P. T.; Mitchell, J. F. *J. Am. Chem. Soc.* **1986**, *108*, 6382. (d) McCullough, L. G.; Schrock, R. R.; Dewan, J. C.; Murdzek, J. C. *J. Am. Chem. Soc.* **1985**, *107*, 5987. (e) Buhro, W. E.; Chisholm, M. H. *Adv. Organomet. Chem.* **1987**, *27*, 311. (f) Bryndza, H. E.; Tam, W. *Chem. Rev.* **1988**, *88*, 1163. (g) Mehrotra, R. C. *Adv. Inorg. Chem. Radiochem.* **1983**, *26*, 269.

(2) (a) Hubert-Pfalzgraf, L. G. *New J. Chem.* **1987**, *11*, 633. (b) Mehrotra, R. C. *J. Non-Cryst. Solids* **1988**, *100*, 1. (c) Guglielmi, M.; Carturan, G. *J. Non-Cryst. Solids*, **1988**, *100*, 16. (d) Brinker, C. J. *J. Non-Cryst. Solids* **1988**, *100*, 31. (e) Schmidt, H. *J. Non-Cryst. Solids* **1988**, *100*, 51. (f) Sanchez, C.; Livage, J.; Henry, M.; Babonneau, F. *J. Non-Cryst. Solids* **1988**, *100*, 65. (g) Rao, C. N. R.; Gopalakrishnan, J. *Acc. Chem. Res.* **1987**, *20*, 228. (h) Mazdiyasni, K. S.; Lynch, C. T.; Smith, J. S. *J. Am. Ceram. Soc.* **1965**, *48*, 372. (i) Aldinger, F.; Kalz, H.-J. *Angew. Chem., Int. Ed. Engl.* **1987**, *26*, 371. (j) Ulrich, D. R. In *Transformation of Organometallics into Common and Exotic Materials: Design and Activation*; Laine, R. M., Ed.; Martinus Nijhoff Publishers: Dordrecht, The Netherlands, 1988; p 207.

(3) (a) Abe, Y.; Kijima, I. *Bull. Chem. Soc. Jpn.* **1970**, *43*, 466. (b) Abe, Y.; Hayama, K.; Kijima, I. *Bull. Chem. Soc. Jpn.* **1972**, *45*, 1258.

(4) Varma, I. D.; Mehrotra, R. C. *J. Prakt. Chem.* **1959**, *8*, 235.

0020-1669/90/1329-2228$02.50/0